

Many body effects and cluster state quantum computation in strongly interacting systems of photons

Dimitris G. Angelakis,¹ Sougato Bose,² Alastair Kay,³ and Marcelo F. Santos⁴

¹*Science Department, Technical University of Crete, Chania, Crete, Greece, 73100*

²*Department of Physics and Astronomy, University College London, Gower St., London WC1E 6BT, UK*

³*Centre for Quantum Computation, Department of Applied Mathematics and Theoretical Physics, University of Cambridge, Wilberforce Road, CB3 0WA, UK*

⁴*Dept. de Física, Universidade Federal de Minas Gerais, Belo Horizonte, 30161-970, MG, Brazil*

We discuss the basic properties of a recently proposed hybrid light-matter system of strongly interacting photons in an array of coupled cavities each doped with a single two level system. Using the non-linearity generated from the photon blockade effect, we predict strong correlations between the hopping photons in the array, and show the possibility of observing a phase transition from a polaritonic insulator to a superfluid of photons. In the Mott phase, this interaction can be mapped to an array of spins. We show how the remaining Hamiltonian, in conjunction with individual spin manipulation, can thus be used for simulating spin chains (useful for state transfer protocols) and cluster state quantum computation.

I. INTRODUCTION

The intractability of simulating coherent many-body phenomena on a classical computer is a major barrier to our understanding of many condensed-matter systems and their dynamics, such as Mott to superfluid phase transitions, high-temperature superconductivity, and anti-ferromagnetism. One of Feynman's great insights was that this problem could be overcome by using other quantum systems, over which we have a much greater degree of control, as simulators.

Cold atoms in optical lattices have been one of the most successful quantum simulators so far [1, 2, 3, 4, 5]. However it is still extremely interesting to explore which other systems permit such phases and simulations, especially as the problem of accessibility of the individual sites has been extremely difficult to address. Here, we review the properties of a recently proposed system which consists of an array of coupled cavities, each doped with a single two-level system. Coupled cavities arrays (CCAs) have been initially proposed for the implementation of quantum gates [6]. In [7] we showed that the atom-cavity interaction could induce a non-linear interaction, commonly described as the photon blockade effect [8, 9], enabling the prediction of strong correlations between the hopping photons in the array. Similarly to optical lattices, which demonstrate a superfluid to Mott insulator phase transition [2], a phase transition was predicted between a superfluid of photons and a Mott phase of hybrid light-matter excitations known as polaritons. Simultaneously and independently with [7], a similar study for strongly interacting polaritons appeared [10]. In this paper we will discuss how hybrid light-matter excitations in CCAs can be used to simulate Mott transitions and XX spin models and how to achieve various quantum information tasks such as quantum state transfer and cluster state quantum computation [7, 11]. We note that, intense interest has arisen since the above early papers that lead to a plethora of studies on various properties of CCAs in the direction of many body simulations [12, 13, 14, 15, 16], production of photonic and steady state entanglement [17, 18] and quantum spin models [19, 20, 21].

II. SYSTEM DESCRIPTION

Consider a chain of N coupled cavities [22, 23]. A realization of this has been studied in structures known as a coupled resonator optical waveguide (CROWs) or coupled cavity waveguides (CCW) in photonic crystals, in tapered fibre-coupled toroidal microcavities and coupled superconducting microwave resonators [24, 25, 26, 27]. The Hamiltonian corresponds to a series quantum harmonic oscillators coupled through hopping photons and is given by $H = \sum_{k=1}^N \omega_d a_k^\dagger a_k + \sum_{k=1}^N A(a_k^\dagger a_{k+1} + H.C.)$, where a_k^\dagger (a_k) are the localized eigenmodes (Wannier functions), i.e. they describe the creation and annihilation of photons within individual cavities. The photon frequency and hopping rate are ω_d and A respectively. There is no non-linearity present yet since we have not introduced a doping.

The cavities are doped by introducing a single two-level system (atoms/ quantum dots/superconducting qubits) to each cavity, which, at site k , have ground and excited states $|g\rangle_k$ and $|e\rangle_k$ respectively [28, 29, 30, 31, 32, 33, 34, 35, 36]. The excited state is at an energy ω_0 above that of the ground state. The resultant Hamiltonian that describes the full system is the sum of three terms; H^{free} the Hamiltonian for the free light and dopant parts, H^{int} the Hamiltonian describing the internal coupling of the photon and dopant in a specific cavity and H^{hop} for the light hopping between

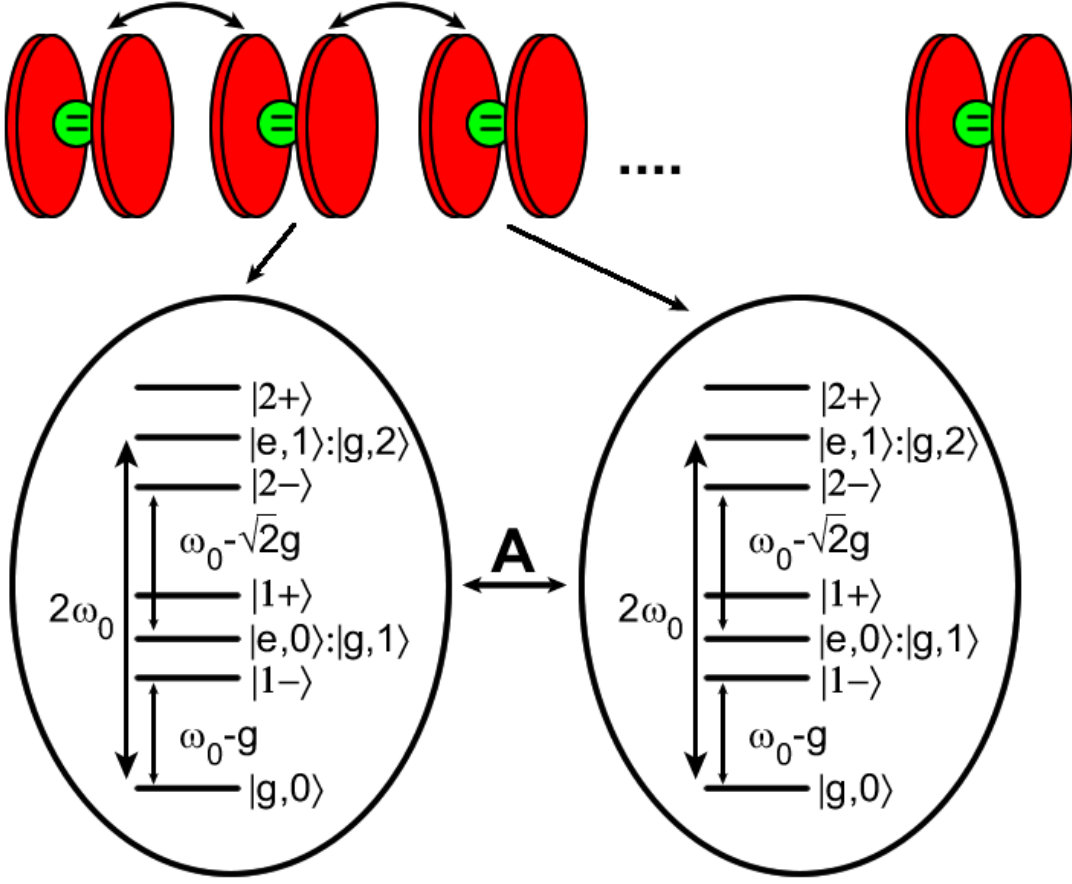


FIG. 1: A series of coupled cavities coupled through light and the polaritonic energy levels for two neighbouring cavities.

cavities.

$$H^{free} = \omega_d \sum_{k=1}^N a_k^\dagger a_k + \omega_0 \sum_k |e\rangle_k \langle e|_k \quad (1)$$

$$H^{int} = g \sum_{k=1}^N (a_k^\dagger |g\rangle_k \langle e|_k + H.C.) \quad (2)$$

$$H^{hop} = A \sum_{k=1}^N (a_k^\dagger a_{k+1} + H.C.) \quad (3)$$

g is the light atom coupling strength. The $H^{free} + H^{int}$ part of the Hamiltonian can be diagonalized in a basis of mixed photonic and atomic excitations, called *polaritons*. These polaritons, also known as dressed states, involve a mixture of photonic and atomic excitations and are defined by the operators $P_k^{(\pm, n)} = |g, 0\rangle_k \langle n \pm |_k$ where $|n\rangle_k$ denote the n photon Fock state in the k th cavity. The polaritons of the k th atom-cavity system, denoted by $|n\pm\rangle_k$, are given by $|n+\rangle_k = (\sin \theta_n |g, n\rangle_k + \cos \theta_n |e, n-1\rangle_k) / \sqrt{2}$ and $|n-\rangle_k = (\cos \theta_n |g, n\rangle_k - \sin \theta_n |e, n-1\rangle_k) / \sqrt{2}$ with energies $E_n^\pm = n\omega_d \pm g\sqrt{n + \Delta^2/g^2}$, $\tan(2\theta_n) = -g\sqrt{n}/\Delta$ and atom-light detuning $\Delta = \omega_0 - \omega_d$. They are also eigenstates of the the sum of the photonic and atomic excitations operator $\mathcal{N}_k = a_k^\dagger a_k + |e\rangle \langle e|_k$ with eigenvalue n (Fig. 1).

A. Polaritonic Mott State

We will now justify that the lowest energy states of the system consistent with a given (integer) number of net excitations per site (or filling factor) becomes a Mott state of the net (polaritonic) excitations. To understand this,

we rewrite the Hamiltonian (for $\Delta = 0$) in terms of the polaritonic operators as

$$\begin{aligned}
H = & \sum_{k=1}^N \left[\sum_{n=1}^{\infty} n(\omega_d - g) P_k^{(-,n)\dagger} P_k^{(-,n)} + \sum_{n=1}^{\infty} n(\omega_d + g) P_k^{(+,n)\dagger} P_k^{(+,n)} + \right. \\
& \left. \sum_{n=1}^{\infty} g(n - \sqrt{n}) P_k^{(-,n)\dagger} P_k^{(-,n)} + \sum_{n=1}^{\infty} g(\sqrt{n} - n) P_k^{(+,n)\dagger} P_k^{(+,n)} \right] + \\
& A \sum_{k=1}^N (a_k^\dagger a_{k+1} + H.C). \tag{4}
\end{aligned}$$

The above implies (assuming the regime $An \ll g\sqrt{n} \ll \omega_d$) that the lowest energy state for a given number, say η , of net excitations at the k th site would be the state $|\eta-\rangle_k$ (this is because $|\eta+\rangle$ has a higher energy, but same net excitation η). Thus one need only consider the first, third and last lines of the above Hamiltonian H for determining the lowest energy states. The first line corresponds to a linear spectrum, equivalent to that of a harmonic oscillator of frequency $\omega_d - g$. If only that part was present in the Hamiltonian, then it would not cost any extra energy to add an excitation (of frequency $\omega_d - g$) to a site already filled with one or more excitations, as opposed to an empty site. However, the term $g(n - \sqrt{n}) P_k^{(-,n)\dagger} P_k^{(-,n)}$ raises energies of uneven excitation distribution such as $|(n+1)-\rangle_k |(n-1)-\rangle_l$ among any two sites k and l relative to the uniform excitation distribution $|n-\rangle_k |n-\rangle_l$ among these sites. Thus the third line of the above Hamiltonian can be regarded as an effective non-linear ‘‘on-site’’ *photonic repulsion*, and leads to a Mott state of the net excitations per site being the ground state for commensurate filling. Reducing the strength of the effective non-linearity, i.e., the blockade effect through detuning for example, should drive the system to the superfluid regime. This could be done by Stark shifting the atomic transitions from the cavity by an external field. The new detuned polaritons are not as well separated as before and their energies are merely shifts of the bare atomic and photonic ones by $\pm g^2 n / \Delta$ respectively. In this case it costs no extra energy to add excitations (excite transitions to higher polaritons) in a single site, and the system moves to the superfluid regime. Note here that the mixed nature of the polaritons could in principle allow for mostly photonic excitations and a photonic Mott state. The required values of g and Δ for the corresponding non-linearity though seem to be unrealistic within current technology [28, 29, 30, 31, 32, 33, 34, 35, 36].

To quantify the transition of the system from a Mott phase to a superfluid phase as the detuning $\Delta = \omega_0 - \omega_d$ is increased, we have performed a numerical simulation of the Hamiltonian of Eqns.(1)-(3) using between 3 and 7 sites (numerical diagonalization of the complete Hamiltonian without any approximations) [50]. In the Mott phase the particle number per site is fixed and its variance is zero (every site is in a Fock state). In such a phase, the expectation value of the destruction operator for the relevant particles, the order parameter, is zero. In the traditional mean field (and thus necessarily approximate) picture, this expectation value becomes finite on transition to a superfluid, as a *coherent* superposition of different particle numbers is allowed to exist per site. However, our entire system is a ‘‘closed’’ system and there is no particle exchange with outside. Superfluid states are characterized by a fixed ‘‘total’’ number of particles in the finite site system and the expectation of a destruction operator in any given site is zero even in the superfluid phase. Thus this expectation value cannot be used as an order parameter for a quantum phase transition. Instead we use the variance of total number of excitations per site, the operator \mathcal{N}_k , in a given site (we choose the middle cavity, but any of the other cavities would do) to characterize the Mott to superfluid phase transition. This variance $var(\mathcal{N}_k)$ has been plotted in Fig.2 as a function of $\log_{10} \Delta$ for a filling factor of one net excitation per site. For this plot, we have taken the parameter ratio $g/A = 10^2$ ($g/A = 10^1$ gives very similar results), with Δ varying from $\sim 10^{-3}g$ to $\sim g$ and $\omega_d, \omega_0 \sim 10^4g$. We have plotted both ideal graphs (if neither the atoms nor the cavity fields undergo any decay or decoherence) and also performed simulations *explicitly* using decay of the atomic states and photonic states in the range of $g/\max(\kappa, \gamma) \sim 10^3$, where κ and γ are cavity and atomic decay rates.

These decay rates are expected soon to be feasible in toroidal microcavity systems with atoms [30] and arrays of coupled stripline microwave resonators, each interacting with a superconducting qubit [33]. For these simulations we have assumed that the experiment (of going from the Mott state to the superfluid state and back) takes place in a time-scale of $1/A$ so that the evolution of one ground state to the other and back is adiabatic. The simulations of the state with decay have been done using quantum jumps, and it is seen that there is *still a large difference of $var(\mathcal{N}_k)$ between the Mott and superfluid phases despite the decays*. As expected the effect of dissipation reduces the final value of order parameter in the superfluid regime (population has been lost through decay) whereas in the Mott regime leads to the introduction of fluctuations, again due to population loss from the $|1-\rangle$ state. The Mott ($var(\mathcal{N}_k) = 0$) to superfluid ($var(\mathcal{N}_k) > 0$) transition takes place over a finite variation of Δ (because of the finiteness of our lattice) around $10g$ and as expected becomes sharper as the number of sites is increased.

In an experiment one would start in the resonant (Mott) regime with all atom-cavity systems initially in their

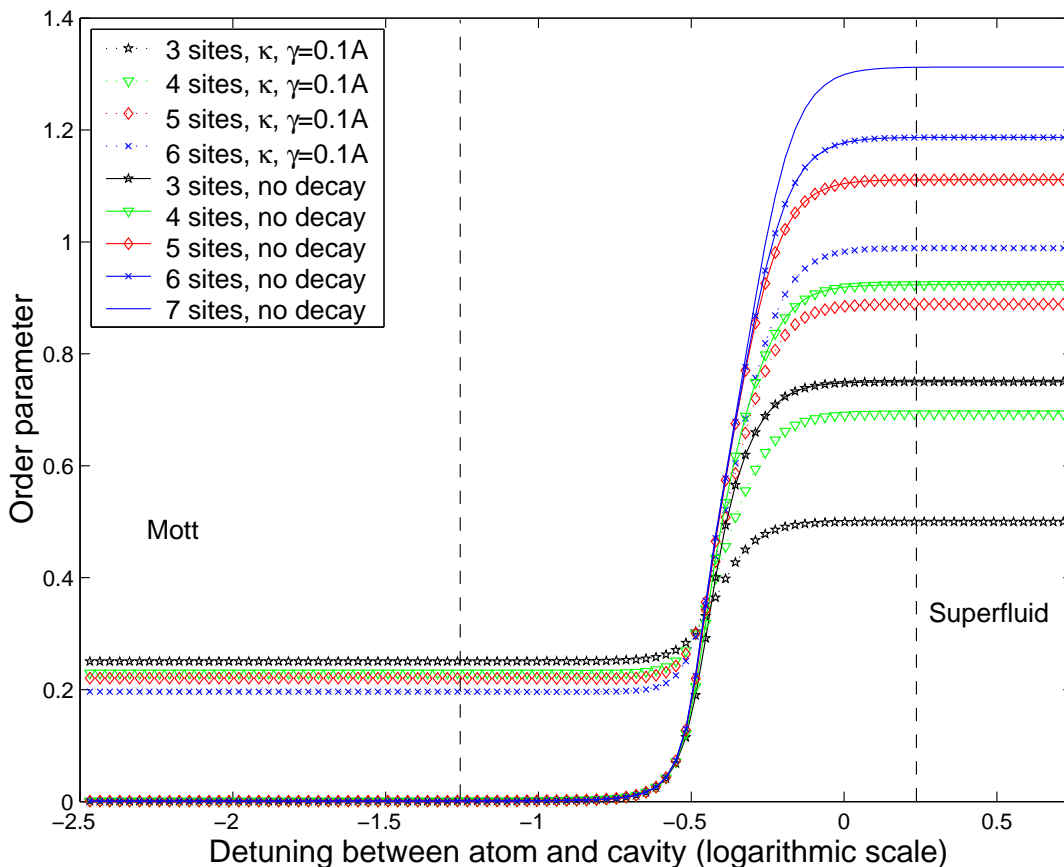


FIG. 2: The order parameter as a function of the detuning between the hopping photon and the doped two level system (in logarithmic units of the matter-light coupling g). Simulations include results for 3-7 sites, with and without dissipation due to spontaneous emission and cavity leakage. Close to resonance ($0 \leq \Delta/g \leq 10^{-1}$), where the photon blockade induced non-linearity is maximum (and much larger than the hopping rate), the system is forced into a polaritonic Fock state with the same integral number of excitations per site (order parameter zero-Mott insulator state). Detuning the system by applying external fields and inducing Stark shifts ($\Delta \geq g$), weakens the blockade and leads to the appearance of different coherent superpositions of excitations per site (a photonic superfluid). The increase in number of sites leads to a sharper transition, as expected.

absolute ground states ($|g, 0\rangle^{\otimes k}$) and prepare the atom-cavity systems in the joint state $|1-\rangle^{\otimes k}$ by applying a global external laser tuned to this transition. This is the Mott state with the total (atomic+photonic) excitations operator \mathcal{N}_k having the value unity at each site. One would then Stark shift and detune (globally again) the atomic transitions from the cavity by an external field and observe the probability of finding each cavity in $|1-\rangle$ and the predicted decrease of this probability (equivalent to the increase in our order parameter, the variance of \mathcal{N}_k) as the detuning is increased. For inferring the fluctuations in \mathcal{N}_k of our system, it suffices to check the population of the $|1-\rangle$ state as this is the only way a single excitation can be present in the k th site. For this, a laser is applied which is of the right frequency to accomplish a cycling transition between $|1-\rangle$ and another, probe, level whose fluorescence can be monitored, giving accurate state measurements [37].

III. SIMULATING XY SPIN MODELS

We will now show that in the Mott regime the system simulates an XY spin model with the presence and absence of polaritons corresponding to spin up and down. Let us assume we initially populate the lattice only with polaritons of energy $\omega_0 - g$. In the limit $\omega_d \approx \omega_0$, Eqs. (4) becomes

$$H_k^{free} = \omega_d \sum_{k=1}^N P_k^{(+)\dagger} P_k^{(+)} + P_k^{(-)\dagger} P_k^{(-)} \quad (5)$$

$$H_k^{int} = g \sum_{k=1}^N P_k^{(+)\dagger} P_k^{(+)} - P_k^{(-)\dagger} P_k^{(-)} \quad (6)$$

$$H_k^{hop.} = A \sum_{k=1}^N P_k^{(+)\dagger} P_{k+1}^{(+)} + P_k^{(-)\dagger} P_{k+1}^{(-)} + P_k^{(+)\dagger} P_{k+1}^{(-)} + P_k^{(-)\dagger} P_{k+1}^{(+)} + H.C. \quad (7)$$

where $P_k^{(\pm)\dagger} = P_k^{(\pm,1)\dagger}$ is the polaritonic operator creating excitations to the first polaritonic manifold (Fig. 1). In the rotating wave approximation, Eq. 7 reads (in the interaction picture). $H_I = A \sum_{k=1}^N P_k^{(-)\dagger} P_{k+1}^{(-)} + H.C.$ In deriving the above, the logic requires two steps. Firstly note that the terms of the type $P_k^{(-)\dagger} P_{k+1}^{(+)}$, which inter-convert between polaritons, are fast rotating and they vanish. Secondly, if we create only the polaritons $P_k^{(-)\dagger}$ in the lattice, then the polaritons corresponding to $P_k^{(+)\dagger}$ will never even be created, as the inter-converting terms are vanishing. Thus the term $P_k^{(+)\dagger} P_k^{(+)}$ can also be omitted. Note that because the double occupancy of the sites is prohibited, one can identify $P_k^{(-)\dagger}$ with $\sigma_k^+ = \sigma_k^x + i\sigma_k^y$, where σ_k^x and σ_k^y are standard Pauli operators. Then the Hamiltonian becomes $H_I = \sigma_k^x \sigma_{k+1}^x + \sigma_k^y \sigma_{k+1}^y$ which is the standard XY model of interacting spins with spin up/down corresponding to the presence/absence of a polariton. Note that although this is different to optical lattice realizations of spin models, where instead, the internal levels of a two level atom are used for the two qubit states [5], the measurement could be done using very similar atomic state measurement techniques (utilizing the advantage of larger distances between sites here).

IV. CLUSTER STATE QUANTUM COMPUTATION

Cluster state generation: The typical implementation of cluster state quantum computing [38, 39], requires initializing all qubits in a 2D lattice in the $|+\rangle = (|0\rangle + |1\rangle)/\sqrt{2}$ state and then performing controlled-phase gates (CP) between nearest-neighbours. In the present CCA system, we have no direct two-qubit gate and the available interaction is not of the Ising type, which straightforwardly gives controlled-phase gates, but an ‘always on’ global Hamiltonian coupling of the XY form. Some consideration of similar scenarios has previously been made [40], although these have primarily concentrated on the Heisenberg interaction. In comparison, the technique which we invoke induces entanglement in a more stable way (from the exchange of two effective fermions [41, 42], and hence it is topological in nature), requires fewer control structures but is inapplicable to the case of Heisenberg coupling. Moreover, the strategy that we will outline momentarily is specifically designed to cope with the always-on nature of the interaction – this is an aspect which is often neglected when forming a cluster state either from Hamiltonian interactions such as the Ising model or as the ground state of a Hamiltonian [43]; one must disable the system dynamics once the state has been formed.

This requirement can be realized by combining the system’s natural dynamics with a protocol where some of the available physical qubits are allocated as gate “mediators” and the rest as the logical qubits. The mediator atoms can be Stark shifted on and off resonance from their cavities through the application of an external field, inhibiting the photon hopping and thereby isolating each logical qubit. The same inhibition of couplings will be used to generate the cluster state. We note here that the error introduced in the step is due to a second-order transition between on-resonance qubits (via a dark-passage through the central off-resonant qubit), which is thus suppressed by a factor of order A/Δ , where $\Delta = \omega_d - \omega_0$ is the detuning of the off-resonant cavity.

Before describing the 4-step global gate sequence to create the cluster state, first observe that to generate the control phase, it is enough to localize chains of 3 qubits, let them evolve for a time $t_0 = \pi/(2\sqrt{2}A)$ and then apply a measurement on the middle ‘mediator’ qubit (in the σ^z basis). Depending on the measurement result, $|0\rangle$ or $|1\rangle$, a non-local gate is generated between the remaining two qubits, either $SWAP.(\sigma^z \otimes \sigma^z).CP$ or $SWAP.CP$ respectively [41]. In both cases, the gates in addition to the CP are Clifford gates, and can thus be recorded and taken into account during the measurement-based computation with the help of an efficient classical computation. Alternatively, if the mediator starts in a known state, say $|0\rangle$, then measuring it and post-selecting on the $|0\rangle$ outcome acts as a useful form of error suppression against timing errors (perfectly) and some forms of decoherence (giving some improvement). On failure (the $|1\rangle$ result), we can make use of the techniques from Benjamin et al. [39] to fix the error.

Our sequence to generate the cluster state is initiated by preparing all qubits in the $|+\rangle$ state through the application of global $\pi/2$ pulse. One quarter of the sites will be used as logical qubits and the rest as “mediators” and “off” qubits interchangeably. By tuning qubits “off” (i.e. moving them off resonance with the aid of the Stark effect, creating an energy cost for photon hopping), we control their interaction with their nearest neighbours and separate the array into

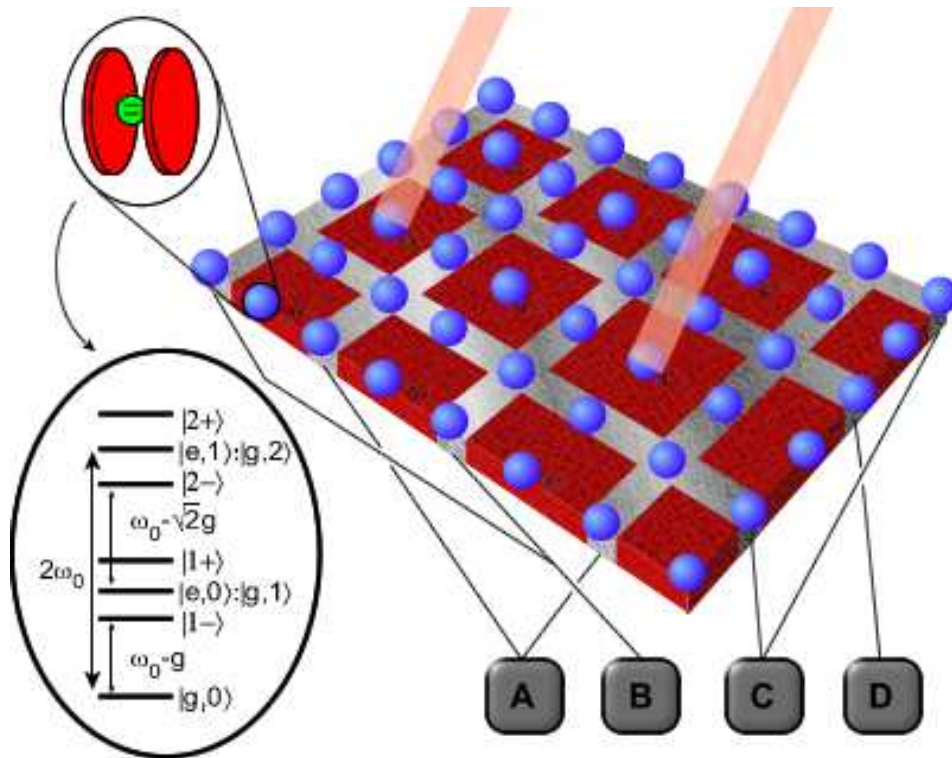


FIG. 3: We work with a 2D array of atom-cavity systems. When the atom is on resonance with the cavity, the ground state $|g, 0\rangle$ and the first excited state $|1-\rangle$ of the combined atom-photon (polaritonic) system in each site can be used as qubits as no other states are accessible[7]. By applying Stark shifts with control electrodes or properly tuned laser fields to sets of qubits (the gates shown under the qubits), we disable the exchange Hamiltonian of a qubit to all of its neighbours creating isolated chains of three qubits. Within each chain, the two extremal qubits are the computational qubits, and the central qubit acts as a mediator. Using only four different groupings of three-qubit chains, we can generate a cluster state. Individual single qubit rotations and measurements are possible and made by properly applying local external fields utilizing the fact that the cavities can be well separated.

chains of three qubits. The steps to create the cluster states are as follows (Fig. 3). First apply gates B, C, D, which take the corresponding systems addressed by them off resonance. By doing this, groups of three ‘on’ qubits are created and isolated from each other. For these we apply the ‘three qubit’ protocol described above and a CP is performed between the extremal qubits of each group. Now for every second line we have every second qubit ‘C-Phased’. In the next step we will connect these pairs to each other by applying A, C, D and the CP protocol again (interchanging the role of previously ‘off’ qubits with mediators). After this stage we have successfully prepared complete rows of qubits in the cluster state. Now we need to connect the columns, which is done by applying the A, B and C gates along with the CP part. Finally, by applying A, B and D, those pairs of columns can be connected, leading to a 2D cluster for every second qubit in the whole array. The required measurement sequence for a particular algorithm is then applied, utilizing the local accessibility of the sites (in any implementation these qubits are at least a few micrometers apart) [28, 29, 30, 31, 32, 33, 34, 35, 36].

As outlined, the initial state of the mediator qubit is irrelevant to the success of the scheme (provided it is in the $|g, 0\rangle, |1-\rangle$ subspace) due to our measurement of it. This protects against decoherence while the atom-cavity system is off resonance. If, instead, we knew that the initial state of the mediator qubit was $|0\rangle$, say, then the measurement would provide a mechanism for low-level error suppression during the application of the gate (projection onto the $|0\rangle$ state leads to the Zeno effect) and detection (if the measurement result is $|1\rangle$). Providing the error probability is small, where small is related to the percolation threshold of the system [38], knowing where these errors occurred allows one to route the computation around the defects. For noisier systems, other techniques can be explored [44].

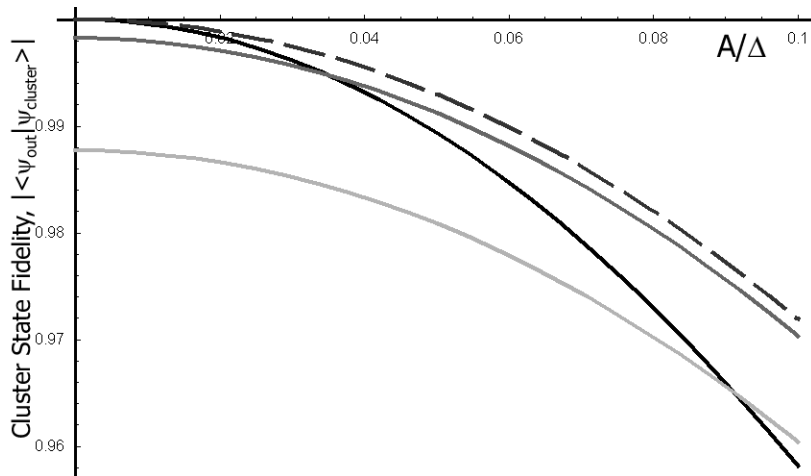


FIG. 4: The fidelity of generation of a cluster state on a 3×3 grid of cavities, as the detuning Δ of the mediator off-resonance cavities is varied (in units of the hopping A). The dashed line includes post-selection on getting $|0\rangle$ outcomes when measuring off-resonance qubits. The grey lines also incorporate spontaneous decay and cavity leakage of $0.05A$ (dark) and $0.08A$ (light).

A. Consideration of Errors

Aside from the aforementioned effect that comes through second-order perturbation theory, which is the primary assumption we have made in deriving the system dynamics, and which results in an error of order A/Δ , what other practical concerns are likely to limit the usefulness of our scheme? Primarily, our concern should be decoherence, which will typically manifest as cavity leakage and spontaneous emission from the atoms. In Fig. 4, we calculate the fidelity of generation of a cluster state on a 3×3 grid of cavities, as the detuning Δ of the mediator off-resonance cavities is varied. The dashed line includes post-selection on getting $|0\rangle$ outcomes when measuring off-resonance qubits, while grey lines also incorporate spontaneous decay and cavity leakage. We observe that the fidelity remains larger than 0.97 even when relatively large values of dissipation are included. More sophisticated schemes have the potential to further reduce the experimental errors. For example, standard Hamiltonian simulation techniques allow us to negate the second order exchange term due to the off-resonance cavities, simply by repeatedly applying σ_z gates to every second on-resonance triplet throughout the evolution. One might even hope that we could use this coherent effect to enhance the scheme through the use of, for example, optimal control techniques. Most of the errors considered here (cavity leakage, spontaneous emission of the atom, and on-off detuning of qubits) are local effects, introducing local noise, which can ultimately be addressed by fault-tolerant techniques [45].

Another class of properties that could be expected to have an effect are timing errors (when the external fields are applied, and how quickly they can be ramped up to maximum strength), and problems with system identification or manufacture. If the system is improperly identified or manufactured, then we will be using an incorrect timescale for the evolution and, as such, it is equivalent to a timing error. Within the difficulties of imperfect system manufacture is the problem of ensuring that the atoms and cavities are on-resonance. However, if they are slightly off resonance, and we can determine this, external fields can be used to compensate. If this is not possible, then, in fact, it does not cause a problem provided the detuning is sufficiently small that we are still within the Mott insulator phase [7], the only difference will be a slight change in the effective coupling between cavities, and hence another timing effect. Thanks to the mediator spin, specifically our ability to measure it, we have a geometric robustness to timing errors [46] i.e. if our timing error is $O(\delta t)$, the accuracy with which the evolution is achieved is only faulty by $O(\delta t^2)$. Finally, the entangling operation, which is the essential part of the whole scheme, has a topological robustness – tuning the parameters of the Hamiltonian differently leaves the generated phase entirely unaffected provided the evolution has completed successfully. Essentially this is a result of the fact that the presence of $|1\rangle$ s in the system can be mapped to the presence of fermions, and it is the topological robustness of the $-ve$ sign appearing when two fermions exchange which we are using [41].

B. Implementing algorithms:

Initial experimental algorithmic implementations with coupled cavities can be expected to utilize the most basic building block of our scheme, a 3×3 grid of cavities, which allows us to generate a four-qubit cluster state. As with the four-photon cluster state initially used by Walther *et al.* and more recently by Pan *et al.*, [47], this cluster state

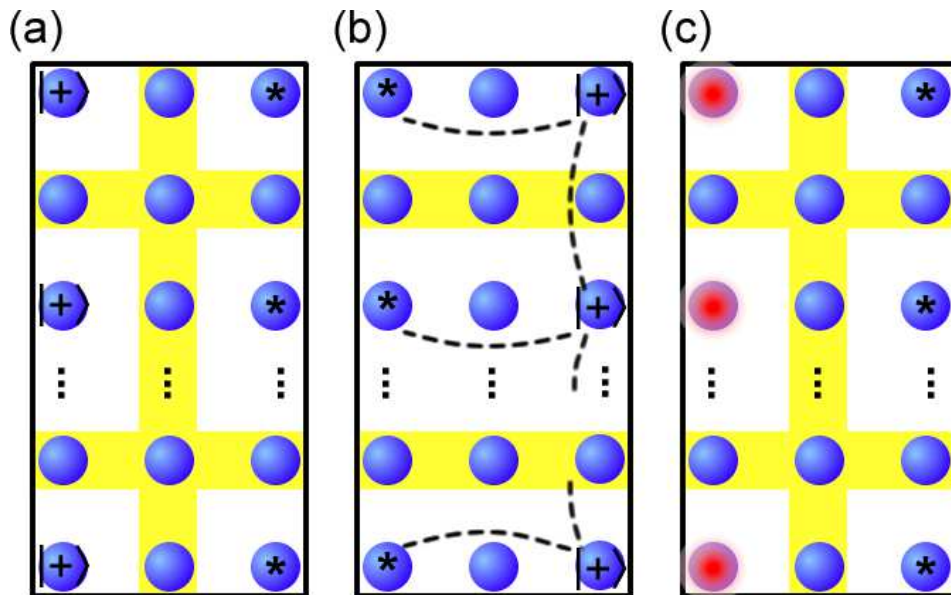


FIG. 5: Sequence for minimising the number of qubits required for a cluster state computation. (a) After the first $n - 1$ steps of the algorithm, the first column of qubits is initialised in the $|+\rangle$ state, and the third column, with qubits denoted by $*$, are in the state of output for the first $n - 1$ steps of the computation. (b) We use control sequences, bringing mediator qubits on resonance, to convert the $|+\rangle$ states into a cluster state, and to entangle them with the output qubits. The SWAP in the entangling operation moves these output qubits to the first column. (c) Measure the qubits of the first column as corresponds to the n^{th} step of the computation, and reinitialise in the $|+\rangle$ state. The rightmost column corresponds to the output. The sequence then repeats.

would be suitable for demonstrating the preparation of an arbitrary one-qubit state, an entangling gate between two qubits, and even the implementation of Grover's search algorithm on two qubits [48]. For example, by applying the local gates $H \otimes H \otimes \sigma_z \otimes \sigma_z$, where H is the Hadamard rotation, we convert of 'box' cluster that the 3×3 grid prepares into the 1D cluster state of 4 qubits, which is given the interpretation of a single qubit, and measurements on the state yield quantum gates on this single qubit. Moreover, generation of this four qubit cluster state is simpler than generation of an arbitrarily sized cluster state because we only need two control steps instead of four, thereby keeping us even further within the decoherence time of the system.

Perhaps the next important step would then be to demonstrate Shor's factoring algorithm, the factoring of 15 being the standard demonstration. To implement as a cluster state computation, the six computational qubits [49] translate into the requirement of a cluster state that is eleven qubits wide. Hence, we need an array which is 21 cavities wide. The breadth of the cluster state, which corresponds to time in the circuit model, is a quantity that we can trade against the time taken for the computation. At one extreme, we can create the whole cluster state in one go, with the simple set of four steps already outlined, and we benefit from the large degree of parallelism available to us. This requires a 2D grid of cavities of size 21×311 [51]. At the other extreme, a grid of 21×3 cavities suffices. In this case, one starts with the 11×2 cluster state, and performs one time step of measurement (i.e. measure the 11 qubits in one column). The result remains in the other column. We then repeat the cluster state generation process, reinitialising the measured qubits in the cluster state, and performing the next time step (Fig. 5). This requires 156 consecutive entangling steps, but the reinitialising of the cluster state after measurement eliminates the effect of decoherence over this timescale. Any combination between these two extremes is also possible, and is a necessary property of any scalable implementation of cluster state computation for the sake of preventing decoherence.

Once initial cluster state experiments have been performed, it simply becomes a question of how many cavities one can reasonably couple together. Alternatively, since the two-qubit gate that we can generate is entangling (and hence universal for quantum computation), we can also consider using it directly to implement the circuit model of computation. This has a much smaller overhead of qubits, but instead requires much higher quality cavities. For example, to factor 15 we would only need a 5×3 grid of cavities to give us six computational qubits. However, we would need approximately 15 consecutive entangling steps (we have attempted to minimise this number by allowing as many of the gates to be applied in parallel as possible, and by optimising the initial labelling of each qubit), hence requiring a time of order $15\pi/(\sqrt{2}A)$. Hence, to reduce the effect of dissipative decay, we require an order of magnitude improvement in the decoherence properties of the qubits to compensate for the increased running time.

V. EXPERIMENTAL IMPLEMENTATIONS

As previously mentioned, there are three primary candidate technologies; fibre coupled micro-toroidal cavities, arrays of defects in PBGs and superconducting qubits coupled through microwave stripline resonators [28, 29, 30, 31, 32, 33, 34, 35, 36]. In order to achieve the required limit of no more than one excitation per site [7], the ratio between the internal atom-photon coupling and the hopping of photons down the chain should be of the order of $g/A \sim 10^2 - 10^1$ (A can be tuned while fabricating the array by adjusting the distance between the cavities and g depends on the type of the dopant). In addition, the cavity/atomic frequencies should be $\omega_d, \omega_0 \sim 10^4 g, 10^5 g$ and the losses should also be small, $g/\max(\kappa, \gamma) \sim 10^3$, where κ and γ are cavity and atom/other decay rates. The polaritonic states under consideration are essentially unaffected by decay for a time $10/A$ (10ns for the toroidal case and 100ns for microwave stripline resonators). While the decay time of $10/A$ may seem uncomfortably close to the preparation time for a cluster state, $\sqrt{2}\pi/A$, the previously described technique (Fig. 5) of continuously reforming the cluster state and connecting it to the output of the previous stage allows a continuous computation that exceeds the decay time for an individual cavity. The required parameter values are currently on the verge of being realised in both toroidal microcavity systems with atoms and stripline microwave resonators coupled to superconducting qubits, but further progress is needed. Arrays of defects in PBGs remain one or two orders of magnitude away, but recent developments, and the integrability of these devices with optoelectronics, make this technology very promising as well. In all implementations the cavity systems are well separated by many times the corresponding wavelength of any local field that needs to be applied in the system for the measurement process.

VI. CONCLUSIONS

In this paper, we showed that a range of many-body system effects, such Mott transitions for polaritonic particles obeying mixed statistics could be observed in optical systems of arrays individually addressable coupled cavities interacting with two level systems. We also showed the capability and advantages of simulating XY spin models using our scheme and noted the ability of these arrays to simulate arbitrary quantum networks. In addition we discussed how universal quantum computation could be realized in a coupled array of individually addressable atom-cavity systems, where the qubits are given by mixed light-matter excitations in each cavity site. While single-qubit operations can be locally achieved, the only available interaction between qubits is due to the natural system Hamiltonian. We show how to manipulate this to give a controlled-phase gate between pairs of qubits. This allows computation either using the circuit model, or a measurement-based computation, the latter being most suited to reducing experimental errors. We have discussed possible architectures for implementing these ideas using photonic crystals, toroidal microcavities and superconducting qubits and point out their feasibility and scalability with current or near-future technology. We also discussed possible implementations using photonic crystals, toroidal microcavities and superconducting systems.

We acknowledge the hospitality of the Centre for Quantum Technologies in NUS, Singapore. This work was supported in part by the E.U. FP6-FET Integrated Project SCALA (CT-015714) and the National Research Foundation & Ministry of Education, Singapore.

-
- [1] M.P.A. Fisher, P.B. Weichman, G. Grinstein, & D.S. Fisher *Phys. Rev. B* **40**, 546-570 (1989).
 - [2] D. Jaksch, C. Bruder, J. I. Cirac, C. W. Gardiner and P. Zoller, *Phys. Rev. Lett.* **81**, 3108 (1997).
 - [3] M. Greiner, O. Mandel, T. Esslinger, T. W. Hänsch and I. Bloch, *Nature* **415**, 39 (2002).
 - [4] Orzel C., et al., *Science* **291**, 2386 (2001).
 - [5] L.-M. Duan, E. Demler and M. D. Lukin, *Phys. Rev. Lett.* **91**, 090402 (2003).
 - [6] Angelakis, D. G., Santos, M. F., Yannopoulos, V. & Ekert, A., *Phys. Lett. A* **362**, 377 (2007).
 - [7] Angelakis, D. G., Santos, M. F. & Bose, S., *Phys. Rev. A* **76**, R05709
 - [8] K. M. Birnbaum, A. Boca et al. *Nature* **436**, 87 (2005).
 - [9] A. Imamoglu, H. Schmidt, et al. *Phys. Rev. Lett.* **79** 1467 (1997).
 - [10] M. J. Hartmann, F. G. S. L. Brandão, and M. B. Plenio, *Nature Phys.* **2**, 849 (2006).
 - [11] D. G. Angelakis and A. Kay, *New J. Phys.* **10** 023012 (2008).
 - [12] A. D. Greentree, C. Tahan, J. H. Cole and L. C. L. Hollenberg, *Nat. Phys.* **2**, 856 (2006).
 - [13] D. Rossini and R. Fazio *Phys. Rev. Lett.* **99**, 186401 (2007).
 - [14] M.X. Xuo, Y. Li, Z. Song and C.P. Sun arXiv:quant-ph/0702078.
 - [15] Y.C. Neil Na, S. Utsunomiya, L. Tian, Y. Yamamoto arXiv:quant-ph/0703219.
 - [16] M. Paternostro, G. S. Agarwal, M. S. Kim, arXiv:0707.0846.
 - [17] J. Cho, D.G. Angelakis, S. Bose arXiv:0712.2413.

- [18] D.G. Angelakis, S. Mancini and S. Bose, arXiv:0711.1830.
- [19] M. J. Hartmann, F. G. S. L. Brandao, and M. B. Plenio, *Phys. Rev. Lett.* **99**, 160501 (2007).
- [20] A. Kay and D. Angelakis, arXiv:0802.0488.
- [21] J. Cho, D. G. Angelakis, S. Bose, arXiv:0802.3365.
- [22] J.M. Raimond, M. Brune, S. Haroche. *Rev. Mod. Phys.* **73** 565 (2001).
- [23] P. Grangier, G. Reymond, & N. Schlosser. *Fortschr. Phys.* **48**, 859 (2000).
- [24] A. Yariv, Y. Xu, R. K. Lee and A. Scherer. *Opt. Lett.* **24**, 711 (1999);
- [25] M. Bayindir, B. Temelkuran and E. Ozbay. *Phys. Rev. Lett.*, **84**, 2140 (2000).
- [26] S. Olivier, C. Smith, M. Rattier, H. Benisty, C. Weisbuch, T. Krauss et al. *Optic. Lett.* **26** 1019, (2001).
- [27] M. Trupke, E.A. Hinds, et al., *Appl. Phys. Lett.* **87**, 211106 (2005).
- [28] Barbosa Alt H., Graef H.-D.C. et al., *Phys. Rev. Lett.* **81** (1998) 4847.
- [29] J. Vuckovic, M. Loncar, H. Mabuchi. & Scherer A. *Phys. Rev. E*, **65**, 016608 (2001).
- [30] D. K. Armani, T. J. Kippenberg, S.M. Spillane & K. J. Vahala. *Nature* **421**, 925 (2003).
- [31] B. Lev, K. Srinivasan, P. Barclay, O. Painter , & H. Mabuchi. *Nanotechnology* **15**, S556, (2004).
- [32] A. Badolato et al, *Science* **308** 1158 (2005).
- [33] A. Wallraff , D. I. Schuster, et al., *Nature* **431**, 162-167 (2004).
- [34] A. Blais, R-S. Huang, et al., *Phys. Rev. A* **69**, 062320 (2004).
- [35] B.-S. Song, S. Noda, et al., *Nat. Mater.* **4**, 207 (2005).
- [36] T. Aoki et al. quant-ph/0606033.
- [37] M.A. Rowe et al., *Nature*, **409**, 791 (2001).
- [38] Raussendorf, R. & Briegel, H. J., *Phys. Rev. Lett.* **86**, 5188 (2001).
- [39] Nielsen, M. A., *Phys. Rev. Lett.* **93**, 040503 (2004); Browne, D. E. & Rudolph, T., *Phys. Rev. Lett.* **95**, 010501 (2005); Barrett, S. D. & Kok, P., *Phys. Rev. A* **71**, 060310(R) (2005); Lim, Y., Beige, A. & Kwek, L., *Phys. Rev. Lett.* **95**, 030505 (2005); Benjamin, S. C., Eisert, J. & Stace, T. M., *New J. Phys.* **7**, 194 (2005); A. Kay, J. K. Pachos & C. S. Adams, *Phys. Rev. A* **73**, 022310 (2006); Blythe P.J. & Varcoe B.T. H, *New J. of Phys.* **8**, 231 (2006); Schön C. et al., *Phys. Rev. Lett.* **11**, 110503 (2005).
- [40] D. Loss and D. P. DiVincenzo. *Phys. Rev. A* **57** 120 (1998); Borhani, M. & Loss, D., *Phys. Rev. A* **71**, 034308 (2005); M. Koniorczyk, P. Rapan and V. Buzek, *Phys. Rev. A* **72**, 022321 (2005).
- [41] Albanese, C., Christandl, M., Datta, N. & Ekert, A., *Phys. Rev. Lett* **93**, 230502 (2004).
- [42] Clark, S., Moura-Alves, C. & Jaksch, D. Efficient generation of graph states for quantum computation. *New J. Phys.* **7**, 124 (2005).
- [43] Bartlett, S. D. & Rudolph, T., *Phys. Rev. A* **74**, 040302(R) (2006).
- [44] Kieling, K., Gross, D. & Eisert, J., Minimal resources for linear optical one-way computing *J. Opt. Soc. Am. B* **24(2)**, 184 (2007).
- [45] Raussendorf, R., Harrington, J. & Goyal, K., An exact effective two-qubit gate in a chain of three spins. *New J. Phys.* **9**, 199 (2007).
- [46] A. Kay, *Phys. Rev. A* **73**, 032306 (2006).
- [47] Walther, P. et al., *Nature* **434**, 169 (2005);
- [48] Lu, C-Y. et al., *Nature Physics* **3**, 91 (2007).
- [49] Lieven, M. K. et al., *Nature* **414**, 883 (2001).
- [50] We use a finite number of sites for the simulation as our system compared to the optical lattices case is computationally more exhaustive. In addition to the bosonic occupation numbers per site there is also the extra atomic degree of freedom at each site that cannot be eliminated [R. Roth and K. Burnett, *Phys. Rev. A* **69**, 021601(R) (2004)].
- [51] To arrive at this required number of gates, we have taken the circuit presented in [49] and converted it into a nearest-neighbor, 2-qubit gate algorithm. Hence, the possibility for some small degree of optimisation in the number of qubits remains.